Since January 2020 Elsevier has created a COVID-19 resource centre with free information in English and Mandarin on the novel coronavirus COVID-19. The COVID-19 resource centre is hosted on Elsevier Connect, the company's public news and information website.

Virology 546 (2020) 88–97

Contents lists available at ScienceDirect

Virology

journal homepage: www.elsevier.com/locate/virology

Antiviral activity of lycorine against Zika virus *in vivo* and *in vitro*

Huini Chen[a,1], Zizhao Lao[b,1], Jiangtao Xu[c,1], Zhaoxin Li[c], Haishan Long[c], Detang Li[d], Luping Lin[e], Xiaohong Liu[f], Liangwen Yu[g,****], Weiyong Liu[h,***], Geng Li[a,c,**], Jianguo Wu[a,*]

[a] Guangdong Key Laboratory of Virology, Institute of Medical Microbiology, Jinan University, Guangzhou, 510632, China
[b] Mathematical Engineering Academy of Chinese Medicine, Guangzhou University of Chinese Medicine, Guangzhou, 510006, China
[c] Laboratory Animal Center, Guangzhou University of Chinese Medicine, Guangzhou, 510006, China
[d] Department of Pharmacy, First Affiliated Hospital of Guangzhou University of Chinese Medicine, Guangzhou, 510405, China
[e] Guangzhou Eighth People's Hospital, Guangzhou Medical University, Guangzhou, 510060, China
[f] The First Affiliated Hospital of Guangzhou University of Chinese Medicine, Guangzhou, 510000, China
[g] Guangzhou University of Chinese Medicine, Guangzhou, 510006, China
[h] Department of Laboratory Medicine, Tongji Hospital, Tongji Medical College, Huazhong University of Science and Technology, Wuhan, China

ARTICLE INFO

Keywords:
ZIKV
Lycorine
Alkaloid
Antiviral
AG6 mice
RdRp inhibitor

ABSTRACT

The emergence and re-emergence of Zika virus (ZIKV), is a cause for international concern. These highly pathogenic arboviruses represent a serious health burden in tropical and subtropical areas worldwide. Despite these burdens, antiviral therapies do not exist, and inhibitors of ZIKV are therefore urgently needed. To elucidate the anti-ZIKV effect of lycorine, we used reverse transcription-quantitative real-time PCR (qRT-PCR), immunofluorescence, Westernwestern blot, and plaque forming assay to analyse viral RNA (vRNA), viral protein, progeny virus counts, and validated inhibitors *in vitro* using a variety of cell lines. Additionally, we found that lycorine acts post-infection according to time-of-addition assay, and inhibits RdRp activity. Lycorine protected AG6 mice against ZIKV-induced lethality by decreasing the viral load in the blood. Due to its potency and ability to target ZIKV infection *in vivo* and *in vitro*, lycorine might offer promising therapeutic possibilities for combatting ZIKV infections in the future.

1. Introduction

Zika virus (ZIKV), first isolated from a rhesus monkey in the Zika forest of Uganda in 1947 (Dick, G W et al., 1952; Routhu, N Kim et al., 2018), is a mosquito-borne, single-stranded, positive-sense RNA arbovirus, and a member of the *Flavivirus* family (Tham et al., 2018). The ZIKV genome encodes three structural proteins (C, prM/M, and E) and seven nonstructural (NS) proteins (NS1, NS2A, NS2B, NS3, NS4A, NS4B, and NS5) (Hamel et al., 2015). ZIKV infection has been associated with several central nervous system diseases, such as Guillain-Barré syndrome, and meningoencephalitis, which are especially harmful to the immature nervous system, and could cause congenital microcephaly in the offspring of pregnant woman (Perez-Cabezas et al., 2019). Scientists have been working on anti-ZIKV research, and most research on drugs is mainly focused on antibody drugs, small-molecule compounds and peptide drugs. Many vaccine candidates have been identified in clinical research, such as DNA vaccines, mRNA vaccines, inactivated virions and viral vectors (Diamond et al., 2019). However, vaccination may cause important issues, such as antibody-dependent enhancement (ADE), and recent FDA approved drug screenings have indicated that many drugs can effectively suppress ZIKV, including candesartan cilexetil (Loe et al., 2019), pinocembrin (Lee et al., 2019), aurintricarboxylic acid (Park et al. 2019), ribavirin and sofosbuvir. However, how to protect pregnant women safely and effectively poses a substantial challenge for the development of small-molecule drugs. Although ribavirin can effectively inhibit ZIKV replication (Kim et al., 2018), it is not yet widely available because it could cause haemolytic anaemia when administered orally over a long term (Russmann et al.,

* Corresponding authors.
** Corresponding author. Guangdong Key Laboratory of Virology, Institute of Medical Microbiology, Jinan University, Laboratory Animal Center, Guangzhou University of Chinese Medicine, Guangzhou, 510006, China.
*** Corresponding authors..
**** Corresponding author.
E-mail addresses: fisherman@gzucm.edu.cn (L. Yu), wyliu@hust.edu.cn (W. Liu), lg@gzucm.edu.cn (G. Li), wu9988@vip.sina.com (J. Wu).
[1] These authors contributed equally to this study.

https://doi.org/10.1016/j.virol.2020.04.009
Received 6 January 2020; Received in revised form 14 April 2020; Accepted 14 April 2020
Available online 19 April 2020

2006). Research has reported that sofosbuvir can also inhibit ZIKV infection (Reznik and Ashby, 2017), but it is not suitable for use in developing countries because of its cost (Bausch et al., 2010).

Lycorine is a benzyl phenethylamine alkaloid, first isolated from *Narcissus pseudonarcissus* in 1877, and [itsthe] structure was elucidated in 1956 (Kornienko and Evidente, 2008). Diverse biological properties have been shown for lycorine, including anticancer (Lamoral-Theys et al., 2010), antiplasmodial (Cedron et al., 2010), antitrypanosomal (Toriizuka et al., 2008), anti-inflammatory (Citoglu et al., 2012), and emetic (Kretzing et al., 2011) properties. Lycorine has also been reported to demonstrate broad-spectrum inhibitory activities against several viruses, such as poliovirus (Hwang et al., 2008), severe acute respiratory syndrome-associated coronavirus (SARS-CoV) (Li et al., 2005), herpes simplex virus (type 1) (Renard-Nozaki et al., 1989), bunyaviruses, Punta Toro virus, and Rift Valley fever virus (Gabrielsen et al., 1992).

Based on our experiments, lycorine may exert potent and effective antiviral activity against ZIKV replication by restraining RdRp activity. In addition, lycorine inhibits hepatitis C virus (HCV) replication by inhibiting the expression of hsc70 in host cells (Chen et al., 2015). Enterovirus 71 (EV71) is suppressed by treatment with lycorine, which interferes with viral polyproteins during elongation (Liu et al., 2011). Furthermore, lycorine inhibits the translocation of the ribonucleoprotein complex from the nucleus in the early stages of influenza virus H5N1 single-cycle and multicycle replication (He et al., 2013). In the present study, we assessed the anti-ZIKV activity of lycorine *in vitro* and *in vivo*. This comprehensive assessment provided new candidate inhibitors to effectively treat ZIKV infections.

2. Materials and methods

2.1. Cells, viruses, and compounds

Vero (African green monkey kidney), Huh7 (hepatocellular carcinoma cells) and A549 (human alveolar basal epithelial adenocarcinoma) cells were grown and maintained in Dulbecco's modified Eagle's medium (DMEM, Thermo Fisher Scientific, Waltham, USA) at 37 °C in 5% CO_2. Drugs were dissolved in 100% dimethylsulfoxide (DMSO, Amresco, Washington, USA) and subsequently diluted in culture medium before each assay. Lycorine (purity > 98%) was purchased from Baoji Chen Guang Biotechnology Company. Asian ZIKV (ZIKV KU963796) was a gift from the Guangdong Provincial Center for Disease Control and Prevention. All cell experiments were performed under the Biological[safety level-2Safety Level-2] (BSL-2) Laboratory.

2.2. Cytotoxicity measurement

Cells were grown at 6×10^3 cells/well in 96-well culture plates and treated with different concentrations of drug. The control group was treated with an equal volume of DMSO. After 48 h, 10% CCK8 reagent was added to each well, the plate was incubated for 1 h and absorbance values were determined at 450 nm. CC_{50} was calculated as the compound concentration required to reduce cell viability by 50%.

2.3. Anti-ZIKV assay

Cells were seeded at 2×10^5 cells/well in 12-well culture plates, and different concentrations of lycorine were added to each well for 2 h. Then, each well was infected with ZIKV at a multiplicity of infection (MOI) of 0.1 for 2 h and incubated until 48 h post infection (hpi). Cells were used to quantitate the vRNA load using qRT-PCR. EC_{50} was calculated as the compound concentration required to reduce viral yields by 50%.

2.4. Immunofluorescence assay

Vero cells were infected with ZIKV at an MOI = 0.1 and treated with lycorine or DMSO. At 48 hpi, the cells were subsequently fixed with 4% paraformaldehyde (Biosharp, Shanghai, China) for 15 min. After fixation, the cells were permeabilized with wash buffer (PBS +0.1% BSA) containing 0.2% Triton X-100 (Amresco, Washington, USA) for 5 min. Then, the cells were blocked with 5% BSA (Beyotime, Jiangsu, China) for 30 min, and the blocking solution was aspirated. The cells were then incubated with the mouse anti-pan flavivirus envelope protein mAb 4G2 (Millipore, Massachusetts, USA) at 4 °C overnight, washed, and incubated with fluorescen-conjugated secondary antibodies at room temperature for 30 min. Cell nuclei were stained using 4',6'-diamidino-2-phenylindole (DAPI, Abbkine, Beijing, China) for 5 min in the dark and imaged by confocal microscopy (Leica, Wetzlar, Germany).

2.5. Plaque forming assay

Vero cells incubated overnight (2×10^5 cells/well) in a 12-well plate were infected with supernatant for 2 h at 37 °C. After incubation, the inoculum was removed, and the cells were immediately replenished with plaque medium supplemented with 1% methylcellulose (Sigma, Saint Louis, USA). Infected cells were incubated for 7 days. After incubation, the plaque medium was removed, and the cells were fixed and stained with 4% formaldehyde and 0.5% crystal violet.

2.6. Time-of-addition assay

Vero cells were seeded in a 12-well plate overnight, and then infected with ZIKV at an MOI = 0.1. Lycorine was added to the well 2 h prior to virus infection or at 0, 1, 2, 4, 6, and 10 hpi, and incubated for up to 48 hpi. Cells were used to quantitate the vRNA load using qRT-PCR. Supernatants were collected for the plaque forming assay.

2.7. Time-of-removal assay

Time-of-removal assay was performed as previously described (Taguwa et al., 2019). Vero cells were infected with ZIKV and either lycorine or DMSO was added at 6 hpi. The level of vRNA synthesis in the presence or absence of drugs was then monitored for up to 24 hpi. Next, the drugs were added at 24 hpi, and the kinetics of ZIKV replication were monitored for an additional 12 h. Cells were used to quantitate the vRNA load using qRT-PCR.

2.8. Detection of ZIKV strand specific RNA by qRT-PCR

Positive- and negative-strand RNA quantification was conducted as previously described with minor modifications(Li et al., 2016). Lycorine (1 μM) and DMSO were added to the culture medium at 24 hpi, and Vero cell was collected at 0, 4, 12, and 24 h for qRT-PCR. The sequences "GGAGGATTCCGGATTGTCAAT" and "TGCCGTGAATCTCA AAAAGGC" were used to obtain cDNA from the negative- (-RNA) and positive-strand (+RNA) RNA, respectively, and qRT-PCR was then performed with primers for strand-specific RNA detection.

2.9. Cellular thermal shift assay (CETSA)

CETSA was conducted as previously described with minor modifications (Yang et al., 2018). Briefly, Vero cells were harvested and rinsed with PBS, and then resuspended in detergent-free buffer (25 mM HEPES, pH 7.0, 20 mM $MgCl_2$, 2 mM DTT) supplemented with protease inhibitors and phosphatase inhibitor cocktail. The cell suspensions were lysed via ultrasound, and subjected to centrifugation at 20,000 × *g* for 20 min at 4 °C to separate the soluble fraction from the cell debris. For the CETSA melting curve experiments, the cell lysates were diluted in

detergent-free buffer and divided into two aliquots, before being treated with or without 20 μM lycorine. After 30 min of treatment at room temperature, each sample was divided into 12 small aliquots at 50 μL/tube, heated individually at different temperatures for 3 min, and immediately cooled for 3 min at room temperature. The heated cell extracts were centrifuged at 20,000 × *g* for 20 min at 4 °C to separate the soluble fractions from the precipitates. After centrifugation, the supernatant was analysed by Westernwestern blotting with an anti-NS5 antibody. The relative chemiluminescence intensities of each sample at different temperatures were used to generate the temperature dependent melting curve. The apparent aggregation temperature (T_{agg}) value was calculated by nonlinear regression.

2.10. In vitro RNA polymerase assays

In vitro RNA polymerase assays were conducted as previously described (Yang et al., 2018). The RNA polymerase assay kit was purchased from Profoldin (Hudson, MA). RNA synthesis assays were performed in 10 μL reactions according to the manufacturer's instructions. After 23 ng of purified ZIKV NS5 was added to a 384-well small-volume plate in 3 μL serial dilutions of lycorine were added to the wells in 3 μL. The mixtures were preincubated for 30 min at room temperature. A master mix containing single-stranded polyribonucleotide,10 μM NTP mix, 20 mM Tris–HCl (pH 8.0), 1 mM DTT, and 8 mM $MgCl_2$ was added to each well in 4 μL. The reactions were incubated at 37 °C for 1 h and then halted by the addition of 10 μL of fluorescent dye. The fluorescence intensities (E_x = 485 ± 5, E_m = 535 ± 10 nm) were measured using a Tecan plate reader.

2.11. Molecular docking

ZIKV RdRp crystal structures were obtained from the Protein Data Bank (PDB). Three-dimensional ligand structures were obtained from the PubChem Compound database and converted into the PDB format using OpenBabel (version 2.4.1). Chem3D Ultra (version 8.0) was used to optimize the ligand structures. Target proteins and optimized ligands were prepared by MGL Tools (version 1.5.6). The binding site and flexible amino acid residues were defined based on previously reported literature. Auto Dock Vina (version 1.1.2) was used in this project to conduct molecular docking analyses. Finally, MGL Tools and Discovery Studio (version 2016) were used to analyse the binding energy and visualize the ligand-protein interactions.

2.12. RNA isolation and qRT-PCR

Cellular vRNA was isolated using a standard protocol (CWBIO, Guangzhou, China), and qRT-PCR assays were performed using SYBR Green (BIO-RAD, California, USA) according to the manufacturer's protocol. Viral RNA expression was calculated using the 2-delta delta CT (cycle threshold) method normalized to GAPDH expression. The absolute animal blood sample copy numbers were derived from the CT values, by reference to a standard curve.

2.13. Western blotting blot analysis

Cells were lysed in CO-IP lysis buffer and centrifuged at 12000 × *g* for 10 min at 4 °C. Proteins were analysed by SDS-PAGE and then transferred to PVDF membranes (Bio-Rad, California, USA). The membranes were blocked with 5% slim milk solution for 1 h and then incubated overnight at 4 °C with primary antibodies. They were then incubated with corresponding secondary antibodies for 1 h. The protein signal was visualized and captured using ECL Western western blot reagent (Bio-Rad, California, USA). Antibodies used to detect the protein expression levels of ZIKV NS5, and E and antibodies for GAPDH were all ordered from Gene Tex (Southern California, USA).

2.14. Animal experiments

This study was approved by the Ethics Committee of Guangzhou University of Chinese Medicine (20190807003). AG6 mice was a gift from Professor Zhao Jincun, State Key Laboratory of Respiratory Diseases, Guangzhou Medical University, China. Four-to five-week old (average 13–15 g), AG6 mice (n = 6 per group) were infected with 3.3×10^6 PFU ZIKV via their footpad, and treated with lycorine (DMSO stock solution diluted with 0.5% carboxymethyl cellulose) at 1, 5, or 10 mg/kg or with an equal volume of 0.5% carboxymethyl cellulose with DMSO. After viral challenge, the treatment was continued for 14 days by intragastric administration. At 1, 3 and 7day post infection (dpi), peripheral blood was taken from the mouse eyeball by retro-orbital puncture for the viremia assay. Brain tissues were collected and the vRNA load was determined by RT–qPCR. Liver and brain tissues were enucleated for pathological section analysis. All animal infection experiments were performed under the Animal Biological Safety Level-2 (ABSL-2) Laboratory.

2.15. Statistical analysis

Statistical analysis was performed using GraphPad Prism 8. Data are reported as the means ± SD. Viral RNA significance analysis was performed using one-way ANOVA, followed by Dunnett's test. P values are indicated in the corresponding figure legends. P values < 0.05 were considered statistically significant.

3. Results

3.1. Quantification of the anti-ZIKV effect of lycorine

To assess the inhibitory properties of lycorine (Fig. 1A), qRT-PCR and plaque forming assay revealed that lycorine inhibits intracellular RNA synthesis and extracellular virion formation (Fig. 1B). Lycorine inhibited plaque formation partially at a concentration of 0.5 μM, and completely at 5 μM (Fig. 1C). Western blotting was performed, after treating Vero cells with 0.01 to 10 μM lycorine. As shown in Fig. 1D, lycorine treatment caused a dose-dependent reduction in the ZIKV protein, and ZIKV envelope biosynthesis was significantly reduced in lycorine-treated cells in a concentration-dependent manner (Fig. 1E).

3.2. Evaluation of antiviral compounds in different cell types

Brequinar, a known pyrimidine synthesis inhibitor, inhibits de novo biosynthesis of uracil nucleotides by inhibiting cellular dihydroxyorotate dehydrogenase (DHODH). Brequinar has strong antiviral activity in viral RNA production and progeny virus production. ZIKV shows the highest sensitivity and low toxicity to brequinar (EC_{50} values of 0.08 μM; $CC_{50} > 50$ μM) (Adcock et al., 2017). Therefore, brequinar was used as positive control. The cytotoxicities and inhibitory activities of lycorine and brequinar in Vero, A549 and Huh7 cells was determined by CCK8 (Dojindo, Kumamoto, Japan) and qRT-PCR, respectively. The cytotoxic concentration 50% (CC_{50}) values and 50% inhibition concentration (EC_{50}) values in Vero cells, A549 cells and Huh7 cells were shown in Table 1. Thus, we concluded that lycorine is a potent inhibitor of ZIKV infection in multiple cell types.

3.3. Time-of-addition assay and mechanism of action study of lycorine

Time-of-addition assay was used to clarify which step of the ZIKV life cycle is affected by lycorine. The qRT-PCR results showed that 1 μM lycorine displayed the strongest ability to decrease the vRNA and viral progeny particle load between -2 and 10 hpi (Fig. 2A). Analysis of the infectious viral proteins in the cells revealed that lycorine reduced viral protein synthesis (Fig. 2B), which coincides with postentry events in the ZIKV replication cycle. Therefore, we hypothesized that lycorine

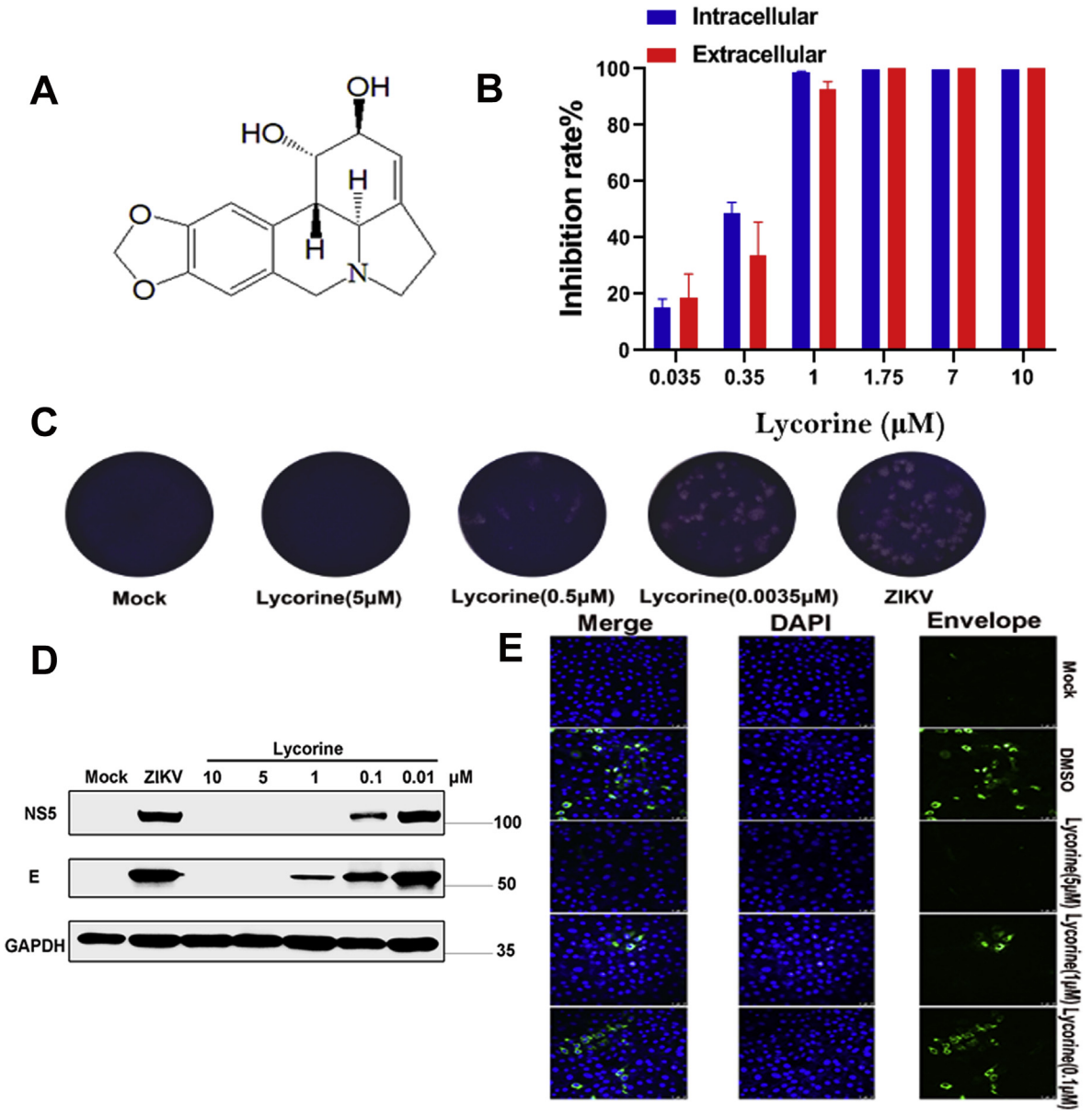

Fig. 1. Dose-dependent inhibition of ZIKV infection by lycorine. (A) The structure of lycorine. (B) Lycorine inhibition of intracellular RNA formation was determined by qRT-PCR, and extracellular virion release was determined by the plaque forming assay. (C) Lycorine inhibition of plaque formation was determined by the plaque forming assay. (D) After ZIKV infection, Vero cells were treated with different concentrations of lycorine and viral protein was detected by $^{\text{Western western}}$ blotting. (E) The antiviral activity of lycorine against ZIKV was determined by an immnofluorescence assay. Cell nuclei were stained with DAPI (blue). Envelope protein was immunostained with an anti-panflavivirus envelope monoclonal antibody (4G2). The envelope protein is indicated in green. . (For interpretation of the references to colour in this figure legend, the reader is referred to the Web version of this article.)

Table 1
Cell cytotoxicity and antiviral activity of lycorine and brequinar.

Cell line	CC_{50} (μM)	Lycorine EC_{50} (μM)	SI	CC_{50} (μM)	Brequinar EC_{50} (μM)	SI
Vero	21	0.39	54	> 50	0.022	> 2272
A549	4.29	0.22	19.5	> 50	0.046	> 1086
Huh7	4.4	0.22	20	> 50	0.006	> 8333

SI: selectivity index.

interferes with the translation and replication of vRNA, and we performed Time-of-removal assay to test this hypothesis. First, lycorine was added at 6 hpi, prior to any significant vRNA synthesis. Compared to DMSO treatment, lycorine treatment fully abrogated vRNA synthesis (Fig. 2C). Next, we added lycorine at 24 hpi and monitored the kinetics of ZIKV replication for an additional 12 h. At this point, viral replication compartments in infected cells are already established. As shown in Fig. 2D, lycorine had no effect on vRNA under these conditions. We also observed similar results for the viral protein level with vRNA (Fig. 2E–2F). Virus E protein was reduced by 52% and NS5 protein was reduced by 89% after 24 h of viral infection (Fig. 2G–2H). Lycorine was added at 24 hpi, no significant difference in viral E and NS5 protein reduction (Fig. 2I–2J). Therefore, we verified that lycorine inhibits the translation and replication of vRNA.

3.4. Lycorine targets the synthesis of ZIKV strand specific RNA

To test the effect of lycorine on the synthesis of positive- and negative-stand RNA, vRNA was isolated for the quantification of positive- and negative-strands. The levels of both positive- and negative-sense

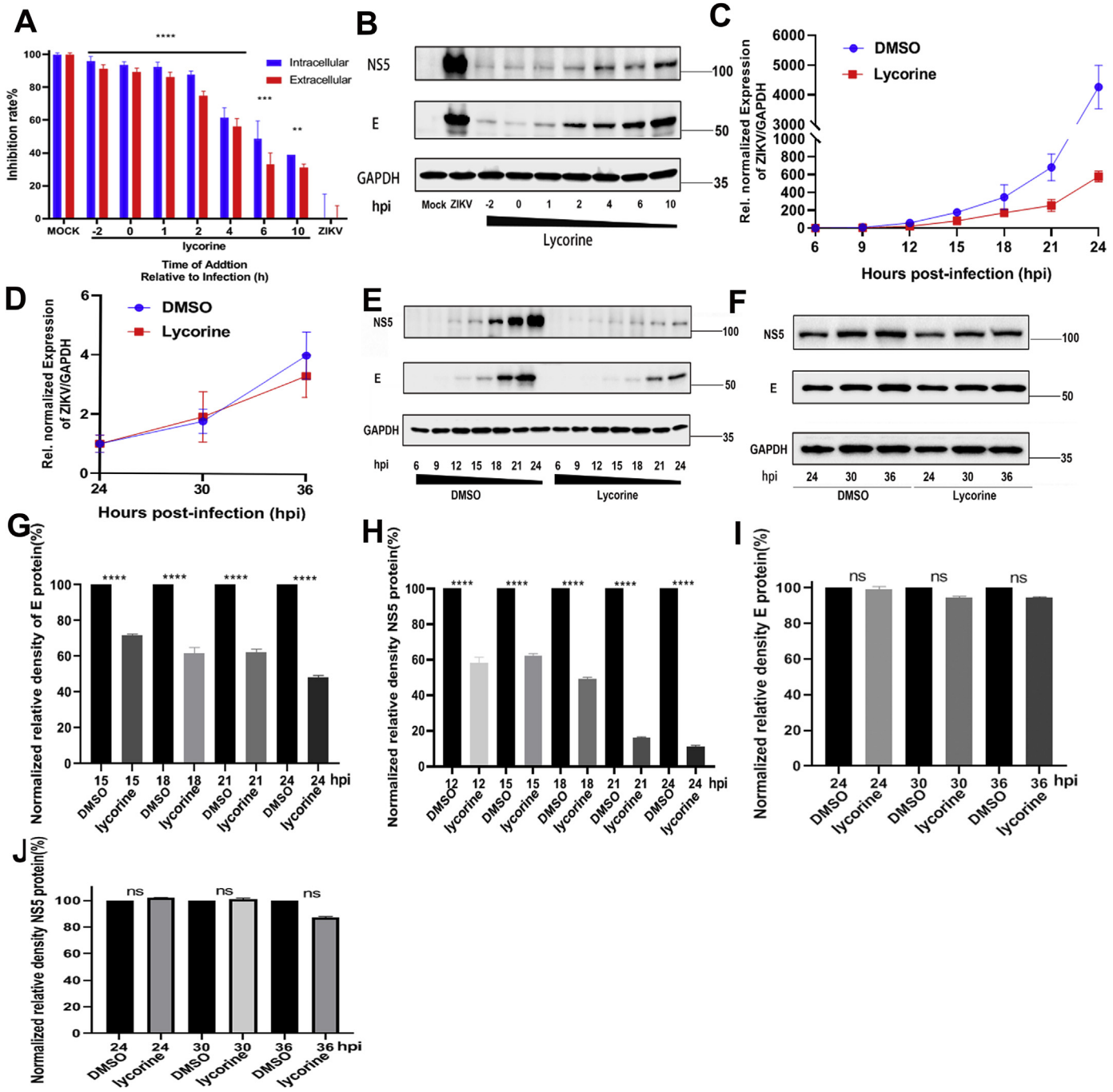

Fig. 2. Lycorine time course and mechanism of action study. (A) Time-of-addition assay. Lycorine (1 μM) was added at -2, 0, 1, 2, 4, 6 and 10 hpi. At 48 hpi, vRNA was measured by qRT-PCR. (B) Viral protein synthesis was determined by $^{\text{Western}}$ $^{\text{western}}$blotting. (C) Time-of-removal assay. At 6 hpi, cells were treated with 1 μM lycorine, and vRNA was monitored every 3 h vRNA was measured by qRT-PCR. (D) At 24 hpi, cells were treated with 1 μM lycorine, and vRNA was monitored every 6 h vRNA was measured by qRT-PCR. (E) Western blot analysis of viral protein expression in at 6 hpi. (F) Western blot analysis of viral protein expression in ZIKV-infected Vero cells after 24 h. (G–H) The intensity quantitation of E and NS5 protein of Fig. 2E. (I–J) The intensity quantitation of E and NS5 protein of Fig. 2F. P ≤ 0.01 (**), P≤0.001 (***), and P ≤ 0.0001 (****).

vRNA were decreased in lycorine treated cells compared to control cells. We compared the efficiency of vRNA synthesis inhibition and found that treated with lycorine inhibited negative- and positive-sense vRNA synthesis by approximately 95% and 93%, respectively (Fig. 3A and B). These observations suggest that lycorine inhibits the synthesis of positive and negative chains during viral replication (Fig. 3C).

3.5. Lycorine binds to ZIKV NS5 and inhibits RdRp activity

CETSA was carried out to examine the direct interactions between lycorine and NS5. T_{agg} values of NS5 in Vero cell lysates were measured in the absence or presence of lycorine at temperatures ranging from 33 to 53.8 °C (Fig. 4A). The CETSA showed that lycorine treatment increased the thermal stability of NS5, markedly increasing the T_{agg} of the NS5 protein from 44.6 to 47.8 °C (Fig. 4B). These results confirmed that lycorine binds directly to NS5 and protects it from thermally induced

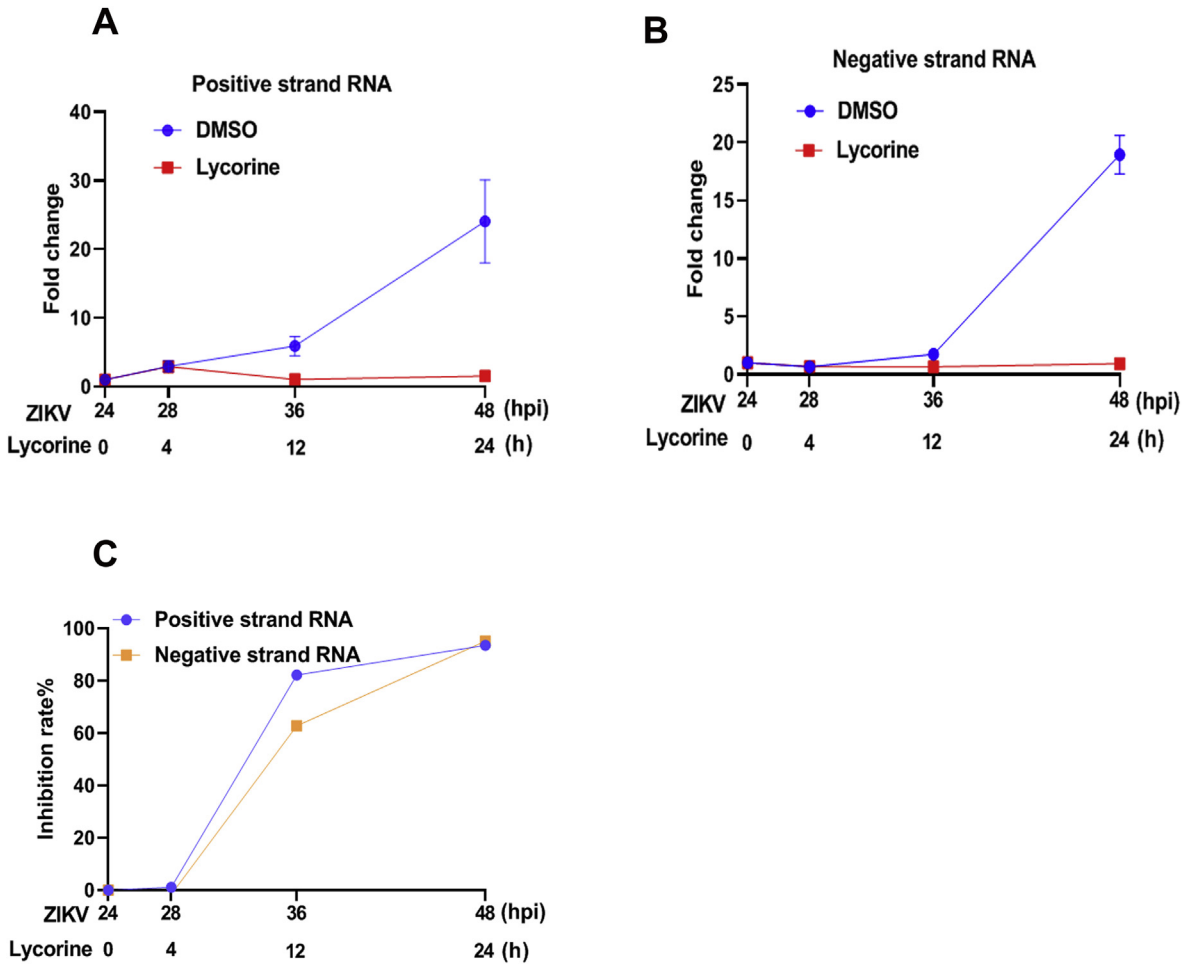

Fig. 3. Lycorine suppresses ZIKV replication by inhibiting the synthesis of positive- and negative-strand vRNA.
Lycorine (1 μM) and DMSO were added to the culture medium at 24 hpi, and the cell were collected at 0, 4, 12, and 24 h for qRT-PCR. (A) Positive-strand RNA. (B) Negative-strand RNA. (C) Efficiency of lycorine on the inhibition of positive-and negative-strand RNA calculated based on the results presented in panels A and B. Data were shown as means ± SD.

aggregation. To further explore whether lycorine inhibits RdRp activity, we performed *in vitro* RNA polymerase assays and found that lycorine directly inhibited RdRp activity in a dose-dependent manner (Fig. 4C). Molecular modelling and docking studies further showed the structural basis of the lycorine binding interactions with ZIKV RdRp (Fig. 4D). The predicted binding model revealed that lycorine preferably bound to the finger domains of RdRp. Together, these results indicated that lycorine targets NS5 and potently inhibits RdRp activity.

3.6. Lycorine protects mice against lethal ZIKV challenge

After infection, mice were treated with lycorine at 1, 5, and 10 mg/kg or with DMSO. As shown in Fig. 5A, the ZIKV group displayed a 100% mortality rate. By 9 dpi, mice in the ZIKV group began to succumb to the infection. In contrast, treatment with lycorine (10 mg/kg) protected against ZIKV infection-induced death by 83%. Lycorine treatment at doses of 5 mg/kg or 1 mg/kg enhanced the survival rates of mice to 66% and 33%, respectively. Mice in the lycorine and ZIKV groups began to lose weight by 5 dpi, those in the lycorine group recovered until 9 or 10 dpi, while those in the ZIKV group did not (Fig. 5B). Viral RNA levels in the blood were quantified in all groups at 1,3 and 7 dpi. In our assay, viremia was observed from 1 dpi, with the highest levels being observed at 3 dpi, however the levels of viremia decreased at 7 dpi. Treatment with 1 mg/kg lycorine inhibited viral replication, but did not prolong the survival times of mice to the same extent as treatment with 5 mg/kg and 10 mg/kg lycorine. The levels of vRNA in the lycorine group were one order of magnitude lower than those in the ZIKV group at 1,3 and 7 dpi. As the concentration of the drug increased, the effect was more pronounced (Fig. 5C–5E). The vRNA load in the brain and liver of mice was performed by RT-qPCR. The experiment showed that 10 mg/kg lycorine reduce the vRNA of brain tissue about three orders of magnitude. 5 mg/kg lycorine reduce the vRNA of brain tissue about one order of magnitude, while 1 mg/kg was not significant difference. As for liver tissue, 10 and 5 mg/kg lycorine reduce the vRNA of liver about one and half order of magnitude, respectively. 1 mg/kg was not significant difference. (Fig. 5F–G). Next, we characterized the histopathological lesion changes in the brain and liver by haematoxylin & eosin staining. In the liver tissue, the cells in the ZIKV group were loosely arranged, and not in the form of strips, while cytoplasmic oedema, and hepatic sinus congestion were observed. Mice in the 10 mg/kg lycorine group displayed significantly reduced liver damage compared to those in the 5 mg/kg lycorine group. The inflammatory response of the cells was obvious in the 1 mg/kg lycorine treatment group. In brain tissues in the ZIKV group, the volume of cells was reduced, the nuclei were shrunken, voids were apparent around the cells and a nuclear membrane was present around the gap. In the 5 mg/kg and 10 mg/kg groups, lycorine significantly reduced the ZIKV-induced inflammatory response. In the 1 mg/kg group, brain tissue lesions were similar to those in the ZIKV group (Fig. 6). Overall, these results confirmed the antiviral effect of lycorine treatment against ZIKV *in vivo*.

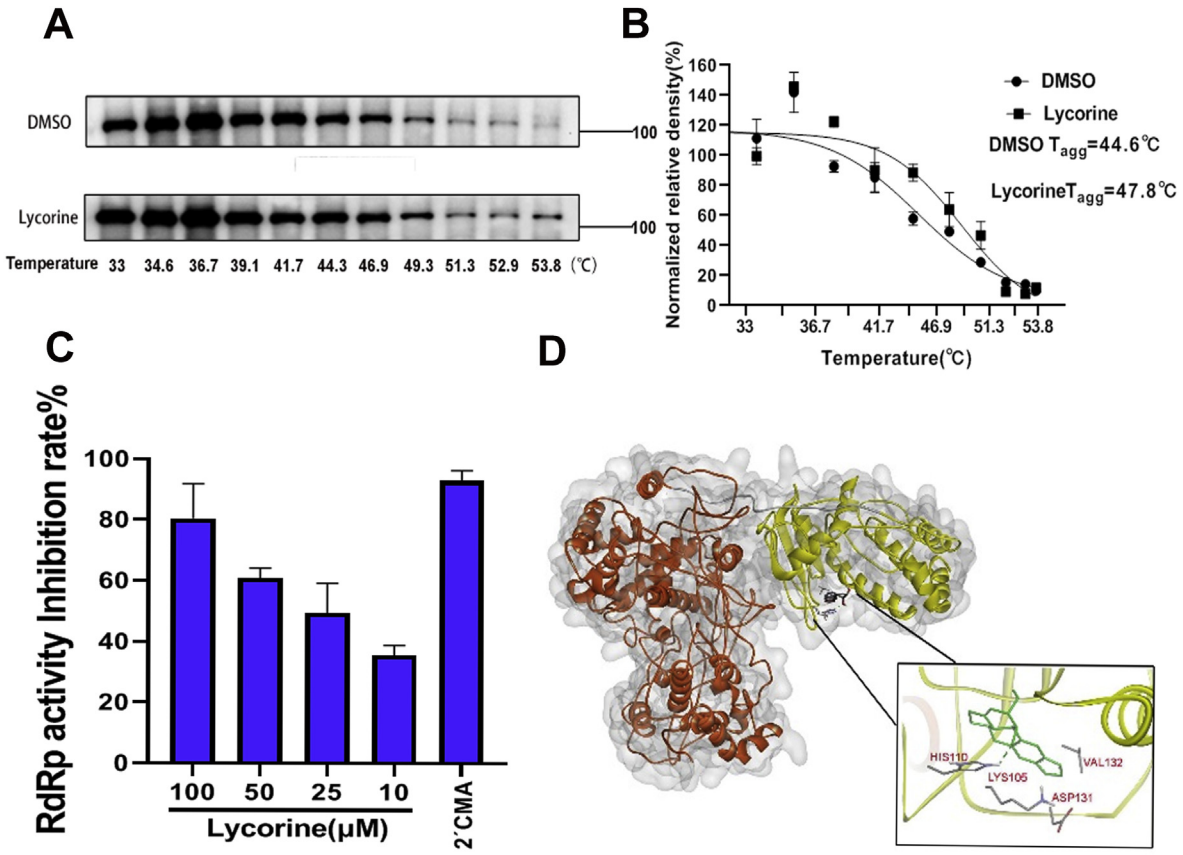

Fig. 4. Lycorine binds to ZIKV NS5 and inhibits RdRp activity. (A) Western blotting showing the ZIKV NS5 CETSA binding assay in the presence or absence of 20 μM lycorine at different temperatures. (B) The NS5 band intensities in the CETSA were quantified and expressed as the means ± SD; n = 3. (C) Dose-response curve showing the inhibitory effect of lycorine treatment on the RdRp activity of recombinant ZIKV NS5 enzyme. 2'CMA (25 μM) was used as a positive control. (D) Predicted model of lycorine binding to ZIKV NS5 RdRp. The RdRp is shown in yellow and the MTase is shown in red. Lycorine binding at the sites are depicted as sticks. A close-up view of the hydrogen-binding interactions of lycorine at the RdRp site is shown. Data were shown as means ± SD. . (For interpretation of the references to colour in this figure legend, the reader is referred to the Web version of this article.)

4. Discussion

ZIKV infection is a serious threat to global health, and there are currently no FDA-approved drugs or licensed vaccines available for the prevention or treatment of ZIKV infection. While antibody-based therapies have shown promise in mouse models, these drugs are expensive, in limited supply, and not validated in humans (Li et al., 2017). Therefore, the discovery of drugs for ZIKV infection remains a priority. In this study, we demonstrated that lycorine has effective and dose-dependent antiviral activity against ZIKV in ZIKV-permissive cell lines, demonstrating that the inhibitory effect of lycorine is not cell-type-specific. Based on the effectiveness of lycorine against ZIKV infection (SI = 54 in Vero cells, 20 in Huh7 cells and 19.5 in A549 cells) compared to that of other previously described drugs, including suramin (SI ~500 in Vero cells) (Tan et al., 2017), BCX4430 (SI = 11.6 in Vero and 15.7 in Huh7 cells) (Julander et al., 2017), and sofosbuvir (SI > 52.63 in Huh7) (Bullard-Feibelman et al., 2017), lycorine is possibly one of the most reasonable options for the treatment of ZIKV infection.

Understanding the roles of lycorine in viral infection may provide insights for drug development. During a single cycle of flavivirus infection, vRNA translation takes place in the first 1 to 5 hpi, vRNA synthesis occurs at ≥ 5 hpi, and progeny virions are released at ≥12 hpi (Chambers et al., 1990). Time-of-addition assay can provide a preliminary understanding of the infectious phase upon which lycorine acts, and results indicate that the compound acts on postentry processes of the ZIKV replication cycle. Time-of-removal assay revealed that lycorine inhibits vRNA and viral protein synthesis at 6 hpi, but has no effect when added at 24 hpi, verifying that lycorine inhibits viral genome formation because viral genome replication requires viral proteins and vRNA.

NS proteins participate in the synthesis of both negative- and positive-sense viral genomes (Cheng et al., 2018). We also found that the synthesis of both negative- and positive-sense vRNA was significantly suppressed by lycorine treatment.

CETSA, which is used to evaluate drug binding to target proteins, is based on the biophysical principle of the ligand-induced thermal stabilization of target proteins (Martinez et al., 2013). One characteristic of the CETSA experiment is the comparison of the melting curve between the control and experimental groups, during which the protein is subjected to a panel of temperatures such that potential thermal stabilization can be assessed (Jafari et al., 2014). The T_{agg} values of NS5 ranged from 44.6 to 47.8 ℃, which shows that lycorine binds to NS5 and protects its stability. NS5 is the largest nonstructural protein, and contains an N-terminal methyltransferase (MTase) domain and a C-terminal RdRp domain(Lin et al., 2019). The RdRp domain, which interacts with other viral and host factors to form a replicase complex responsible for their replication, is required for RNA synthesis and is essential for flavivirus replication. In a previous experiment, we demonstrated that lycorine inhibits the formation of vRNA. Therefore, we designed *in vitro* RNA polymerase assays to verify whether lycorine inhibits RdRp activity, and the experiment results showed that lycorine treatment inhibited RdRp activity. RdRp would be an ideal target option for anti-ZIKV infection because human host cells are devoid of RdRp (Lin et al., 2019). Therefore, further studies are required to define the mechanism by which lycorine acts on RdRp. Lycorine inhibits HCV replication by inhibiting HSP70 (Chen et al., 2015) and EV71A by 2A

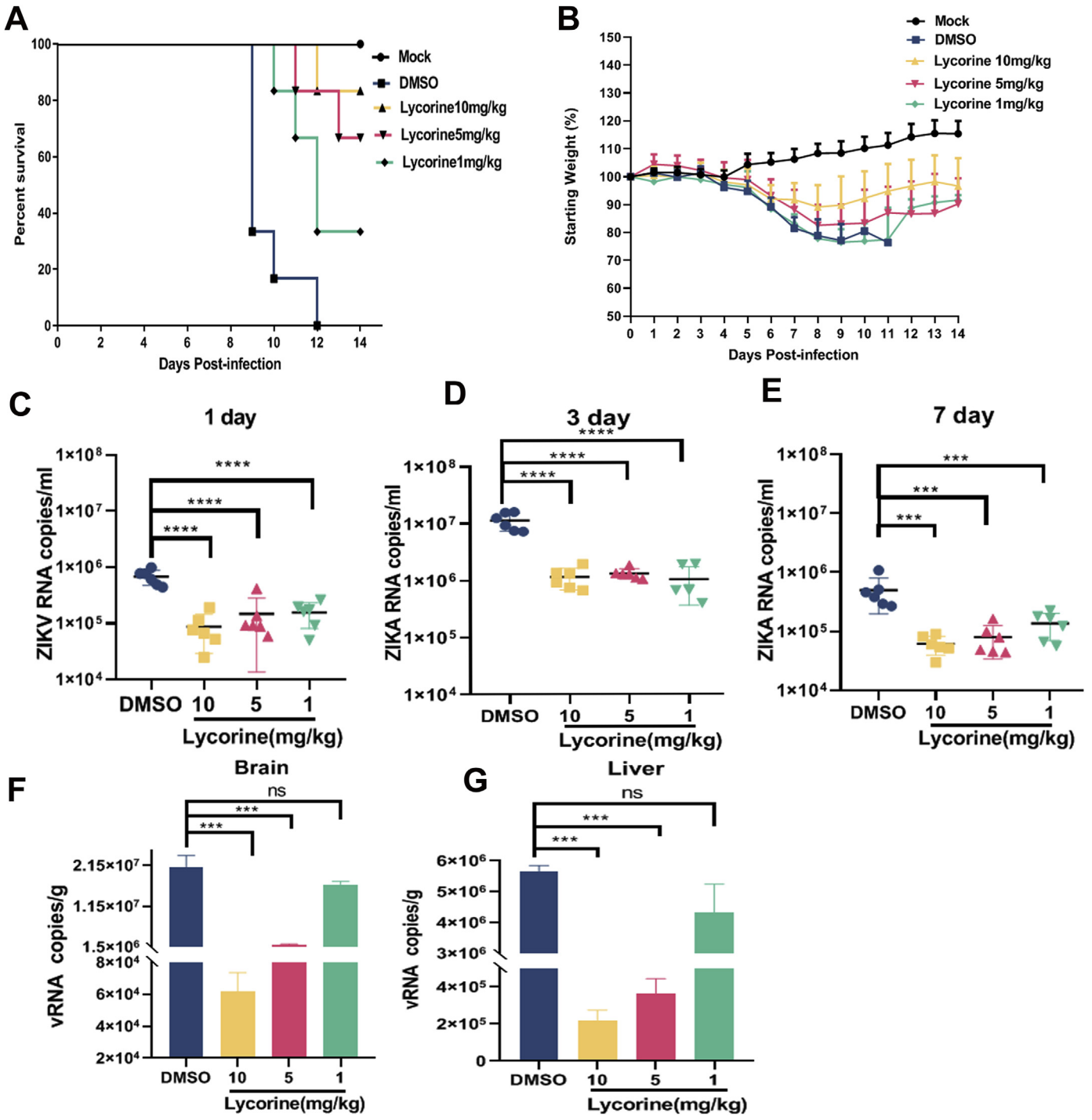

Fig. 5. Lycorine protects mice from ZIKV challenge. (A) Survival rate of mice. (B) Body weight changes of mice measured between 0 and 14 dpi. (C–E) Time-course of vRNA in the sera of the mice collected at 1, 3 and 7dpi, as measured by qRT-PCR. Ct values for the known concentrations of RNA were plotted against the logs of the genome equivalent copy numbers. The resultant standard curve was used to determine the number of ZIKV RNA genome equivalents in the samples. (F–G) Viral RNA load in brain and liver tissue. The vRNA load in brain and liver of mice was determined by RT–qPCR. Data were shown as means ± SD. $P \leq 0.01$ (**), $P \leq 0.001$ (***), and $P \leq 0.0001$ (****).

protease (Guo et al., 2016). HSP70 participates in the formation of virus replication complexes (Taguwa et al., 2019). It is possibility that lycorine may inhibit ZIKV replication by inhibiting HSP70 protein. In this assay, we showed that lycorine inhibited ZIKV replication by inhibiting the activity of RdRp by detecting RdRp activity. RdRp also play a role in the replication of ZIKV (Lu et al., 2017). This suggests that there may be multiple targets for lycorine to inhibit ZIKV replication. 2A protease of EV71A is a homologue of dengue NS3 protein. Dengue NS3 protein is similar to ZIKV NS3 protein (Jain et al., 2016). The NS3 protein is activated by the NS2B protein to form NS2B-NS3 proteolytic enzymes, which are involved in the cleavage of ZIKV polyprotein (White et al., 2016). Because there may be multiple targets for the inhibition of ZIKV by lycorine, we performed molecular docking experiments on the possible targets. As shown in the Table 2, lycorine has the ability to bind to HSP70 and ZIKV NS3 protein, but the stability is weaker than the positive control. So in order to better clarify the effect of lycorine on

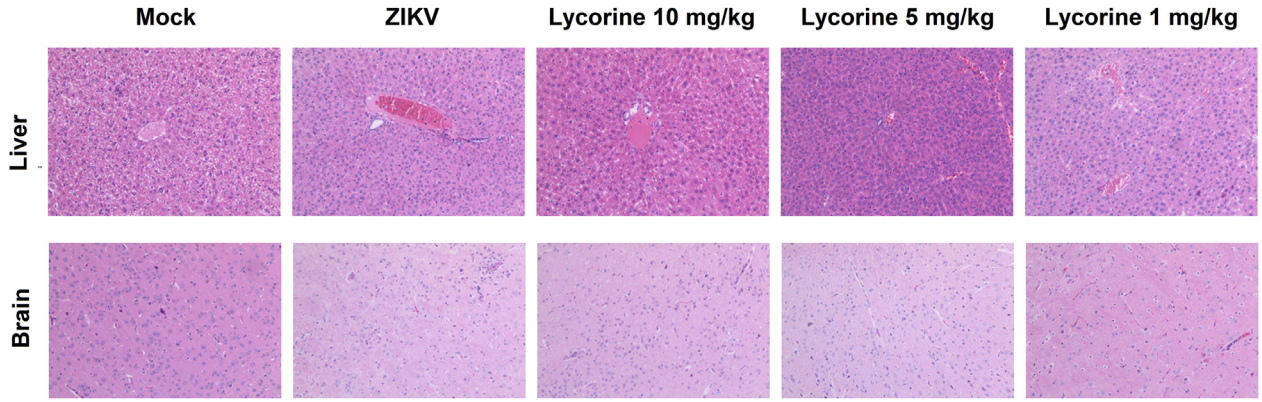

Fig. 6. Lycorine treatment reduces pathological damage in ZIKV-challenged AG6 mice. Haemtoxylin-eosin staining of brain and liver sections from AG6 mice, The magnification is200 × .

Table 2
The binding energy of lycorine with ZIKV NS3 and HSP70.

	ZIKV NS3	HSP70
Lycorine	−8.71	−10.04
ADP		−13.56
NTP	−9.3	

ADP and NTP was as positive control.

HSP70 and ZIKV NS3. More experiments are needed to be.

Animal models are reasonable tools to evaluate the efficacy of antiviral compounds *in vivo*. In our research, the differential effects of lycorine administered at 1 mg/kg, 5 mg/kg and 10 mg/kg may have been due to the fact that 1 mg/kg lycorine does not inhibit ZIKA infection-induced apoptosis and a previous study showed that ZIKV infection induces apoptosis (Park et al. 2019). Another possibility is that the daily administration of a high concentration of lycorine is required to prolong the survival of ZIKV-infected mice. However, the mechanisms underlying the prolonged survival and mortality outcomes of mice remain unknown. One major issues remain to be addressed for the further development of lycorine. It is a lack of knowledge about the its use of lycorine in pregnant women, and additional safety tests are thus required before lycorine can be used for the treatment of pregnant women. An improved animal model that allows a better estimation of the *in vivo* potency of lycorine, including non-human primate models, should be established for a preclinical toxicity study that may be beneficial for understanding the antiviral activity of lycorine for its use as a novel antiviral drug.

5. Conclusion

In summary, we demonstrated that lycorine inhibits ZIKV infection *in vitro* by restraining RdRp activity. Antiviral experiments *in vivo* show that lycorine increases mouse survival and reduces viremia. Our results support lycorine as candidate drug for the ZIKV-infection treatment.

CRediT authorship contribution statement

Huini Chen: Formal analysis. **Zizhao Lao:** Formal analysis. **Jiangtao Xu:** Formal analysis. **Zhaoxin Li:** Formal analysis. **Haishan Long:** Formal analysis. **Detang Li:** Formal analysis. **Luping Lin:** Formal analysis. **Xiaohong Liu:** Formal analysis. **Liangwen Yu:** Formal analysis, Writing - original draft. **Weiyong Liu:** Formal analysis, Writing - original draft. **Geng Li:** Formal analysis, Writing - original draft. **Jianguo Wu:** Formal analysis, Writing - original draft.

Declaration of competing interest

None.

Acknowledgement

This work was generously supported by the Natural Science Foundation of Guangdong Province (2017A030313626), Excellent Young Scholars Project of the First Affiliated Hospital of Guangzhou University of Chinese Medicine (2019QN22 and 2017ZWB10), Science & Technology Planning Project of Guangzhou (201804010029), National Nature Science Foundation of China (81973549,81803813, 81730061, and 81471942), The Open Project of State Key Laboratory of Natural Medicines (SKLNMKF201906), Science & Technology Planning Project of Guangdong Province Office of Education (2014GKXM032), Program of Guangdong Natural Science Foundation of China (S201230006598), Science & Technology Planning Project of Guangdong Province Office of Education (2018KCXTD007), Key Research Projects of GZUCM First-class Universities and Top Disciplines (A1-AFD018191A17), GZUCM First-class Universities and Top Disciplines Scientific Research Team Projects (2019KYTD102), and Guangdong Province “Pearl River Talent Plan” Innovation and Entrepreneurship Team Project (2017ZT07Y580).

References

Adcock, R.S., Chu, Y.K., Golden, J.E., Chung, D.H., 2017. Evaluation of anti-Zika virus activities of broad-spectrum antivirals and NIH clinical collection compounds using a cell-based, high-throughput screen assay. Antivir. Res. 138, 47–56.
Bausch, D.G., Hadi, C.M., Khan, S.H., Lertora, J.J., 2010. Review of the literature and proposed guidelines for the use of oral ribavirin as postexposure prophylaxis for Lassa fever. Clin. Infect. Dis. 51, 1435–1441.
Bullard-Feibelman, K.M., Govero, J., Zhu, Z., Salazar, V., Veselinovic, M., Diamond, M.S., Geiss, B.J., 2017. The FDA-approved drug sofosbuvir inhibits Zika virus infection. Antivir. Res. 137, 134–140.
Cedron, J.C., Gutierrez, D., Flores, N., Ravelo, A.G., Estevez-Braun, A., 2010. Synthesis and antiplasmodial activity of lycorine derivatives. Bioorg. Med. Chem. 18, 4694–4701.
Chambers, T.J., Hahn, C.S., Galler, R., Rice, C.M., 1990. Flavivirus genome organization, expression, and replication. Annu. Rev. Microbiol. 44, 649–688.
Chen, D., Cai, J., Cheng, J., Jing, C., Yin, J., Jiang, J., Peng, Z., Hao, X., 2015. Design, synthesis and structure-activity relationship optimization of lycorine derivatives for HCV inhibition. Sci. Rep. 5, 14972.
Cheng, F., Ramos, D.S.S., Huang, I.C., Jung, J.U., Gao, S.J., 2018. Suppression of Zika virus infection and replication in endothelial cells and astrocytes by PKA inhibitor PKI 14-22. J. Virol. 92.
Citoglu, G.S., Acikara, O.B., Yilmaz, B.S., Ozbek, H., 2012. Evaluation of analgesic, anti-inflammatory and hepatoprotective effects of lycorine from Sternbergia fisheriana (Herbert) Rupr. Fitoterapia 83, 81–87.
Diamond, M.S., Ledgerwood, J.E., Pierson, T.C., 2019. Zika virus vaccine development: progress in the face of new challenges. Annu. Rev. Med. 70, 121–135.
Dick, G.W., Kitchen, S.F., Haddow, A.J., 1952. Zika virus. I. Isolations and serological specificity. Trans. R. Soc. Trop. Med. Hyg. 46, 509–520.
Gabrielsen, B., Monath, T.P., Huggins, J.W., Kefauver, D.F., Pettit, G.R., Groszek, G.,

Hollingshead, M., Kirsi, J.J., Shannon, W.M., Schubert, E.M., Et, A., 1992. Antiviral (RNA) activity of selected Amaryllidaceae isoquinoline constituents and synthesis of related substances. J. Nat. Prod. 55, 1569–1581.
Guo, Y., Wang, Y., Cao, L., Wang, P., Qing, J., Zheng, Q., Shang, L., Yin, Z., Sun, Y., 2016. A conserved inhibitory mechanism of a lycorine derivative against enterovirus and hepatitis C virus. Antimicrob. Agents Chemother. 60, 913–924.
Hamel, R., Dejarnac, O., Wichit, S., Ekchariyawat, P., Neyret, A., Luplertlop, N., Perera-Lecoin, M., Surasombatpattana, P., Talignani, L., Thomas, F., Cao-Lormeau, V.M., Choumet, V., Briant, L., Despres, P., Amara, A., Yssel, H., Misse, D., 2015. Biology of Zika virus infection in human skin cells. J. Virol. 89, 8880–8896.
He, J., Qi, W.B., Wang, L., Tian, J., Jiao, P.R., Liu, G.Q., Ye, W.C., Liao, M., 2013. Amaryllidaceae alkaloids inhibit nuclear-to-cytoplasmic export of ribonucleoprotein (RNP) complex of highly pathogenic avian influenza virus H5N1. Influenza Other Respir Viruses 7, 922–931.
Hwang, Y.C., Chu, J.J., Yang, P.L., Chen, W., Yates, M.V., 2008. Rapid identification of inhibitors that interfere with poliovirus replication using a cell-based assay. Antivir. Res. 77, 232–236.
Jafari, R., Almqvist, H., Axelsson, H., Ignatushchenko, M., Lundback, T., Nordlund, P., Martinez, M.D., 2014. The cellular thermal shift assay for evaluating drug target interactions in cells. Nat. Protoc. 9, 2100–2122.
Jain, R., Coloma, J., García-Sastre, A., Aggarwal, A.K., 2016. Structure of the NS3 helicase from Zika virus. Nat. Struct. Mol. Biol. 23, 752–754.
Julander, J.G., Siddharthan, V., Evans, J., Taylor, R., Tolbert, K., Apuli, C., Stewart, J., Collins, P., Gebre, M., Neilson, S., Van Wettere, A., Lee, Y.M., Sheridan, W.P., Morrey, J.D., Babu, Y.S., 2017. Efficacy of the broad-spectrum antiviral compound BCX4430 against Zika virus in cell culture and in a mouse model. Antivir. Res. 137, 14–22.
Kim, J.A., Seong, R.K., Kumar, M., Shin, O.S., 2018. Favipiravir and ribavirin inhibit replication of asian and african strains of Zika virus in different cell models. Viruses 10.
Kornienko, A., Evidente, A., 2008. Chemistry, biology, and medicinal potential of narciclasine and its congeners. Chem. Rev. 108, 1982–2014.
Kretzing, S., Abraham, G., Seiwert, B., Ungemach, F.R., Krugel, U., Regenthal, R., 2011. Dose-dependent emetic effects of the Amaryllidaceous alkaloid lycorine in beagle dogs. Toxicon 57, 117–124.
Lamoral-Theys, D., Decaestecker, C., Mathieu, V., Dubois, J., Kornienko, A., Kiss, R., Evidente, A., Pottier, L., 2010. Lycorine and its derivatives for anticancer drug design. Mini Rev. Med. Chem. 10, 41–50.
Lee, J.L., Loe, M., Lee, R., Chu, J., 2019. Antiviral activity of pinocembrin against Zika virus replication. Antivir. Res. 167, 13–24.
Li, C., Zhu, X., Ji, X., Quanquin, N., Deng, Y.Q., Tian, M., Aliyari, R., Zuo, X., Yuan, L., Afridi, S.K., Li, X.F., Jung, J.U., Nielsen-Saines, K., Qin, F.X., Qin, C.F., Xu, Z., Cheng, G., 2017. Chloroquine, a FDA-approved drug, prevents Zika virus infection and its associated congenital microcephaly in mice. EBioMedicine 24, 189–194.
Li, S.Y., Chen, C., Zhang, H.Q., Guo, H.Y., Wang, H., Wang, L., Zhang, X., Hua, S.N., Yu, J., Xiao, P.G., Li, R.S., Tan, X., 2005. Identification of natural compounds with antiviral activities against SARS-associated coronavirus. Antivir. Res. 67, 18–23.
Li, X.F., Dong, H.L., Huang, X.Y., Qiu, Y.F., Wang, H.J., Deng, Y.Q., Zhang, N.N., Ye, Q., Zhao, H., Liu, Z.Y., Fan, H., An, X.P., Sun, S.H., Gao, B., Fa, Y.Z., Tong, Y.G., Zhang, F.C., Gao, G.F., Cao, W.C., Shi, P.Y., Qin, C.F., 2016. Characterization of a 2016 clinical isolate of Zika virus in non-human primates. EBioMedicine 12, 170–177.
Lin, Y., Zhang, H., Song, W., Si, S., Han, Y., Jiang, J., 2019. Identification and characterization of Zika virus NS5 RNA-dependent RNA polymerase inhibitors. Int. J. Antimicrob. Agents 54, 502–506.
Liu, J., Yang, Y., Xu, Y., Ma, C., Qin, C., Zhang, L., 2011. Lycorine reduces mortality of human enterovirus 71-infected mice by inhibiting virus replication. Virol. J. 8, 483.
Loe, M., Lee, R., Chu, J., 2019. Antiviral activity of the FDA-approved drug candesartan cilexetil against Zika virus infection. Antivir. Res. 172, 104637.
Lu, G., Bluemling, G.R., Collop, P., Hager, M., Kuiper, D., Gurale, B.P., Painter, G.R., De La Rosa, A., Kolykhalov, A.A., 2017. Analysis of ribonucleotide 5'-triphosphate analogs as potential inhibitors of Zika virus RNA-dependent RNA polymerase by using non-radioactive polymerase assays. Antimicrob. Agents Chemother. 61.
Martinez, M.D., Jafari, R., Ignatushchenko, M., Seki, T., Larsson, E.A., Dan, C., Sreekumar, L., Cao, Y., Nordlund, P., 2013. Monitoring drug target engagement in cells and tissues using the cellular thermal shift assay. Science 341, 84–87.
Park, J.G., Avila-Perez, G., Madere, F., Hilimire, T.A., Nogales, A., Almazan, F., Martinez-Sobrido, L., 2019. Potent inhibition of Zika virus replication by aurintricarboxylic acid. Front. Microbiol. 10, 718.
Perez-Cabezas, V., Ruiz-Molinero, C., Nunez-Moraleda, B., Jimenez-Rejano, J.J., Chillon-Martinez, R., Moral-Munoz, J.A., 2019. Guillain-Barre Syndrome and Zika infection: identifying leading producers, countries relative specialization, and collaboration. FEMS Microbiol. Lett. 366 (5).
Renard-Nozaki, J., Kim, T., Imakura, Y., Kihara, M., Kobayashi, S., 1989. Effect of alkaloids isolated from Amaryllidaceae on herpes simplex virus. Res. Virol. 140, 115–128.
Reznik, S.E., Ashby, C.J., 2017. Sofosbuvir: an antiviral drug with potential efficacy against Zika infection. Int. J. Infect. Dis. 55, 29–30.
Routhu, N.K., Xie, Y., Dunworth, M., Casero, R.J., Oupicky, D., Byrareddy, S.N., 2018. Polymeric prodrugs targeting polyamine metabolism inhibit Zika virus replication. Mol. Pharm. 15, 4284–4295.
Russmann, S., Grattagliano, I., Portincasa, P., Palmieri, V.O., Palasciano, G., 2006. Ribavirin-induced anemia: mechanisms, risk factors and related targets for future research. Curr. Med. Chem. 13, 3351–3357.
Taguwa, S., Yeh, M.T., Rainbolt, T.K., Nayak, A., Shao, H., Gestwicki, J.E., Andino, R., Frydman, J., 2019. Zika virus dependence on host Hsp70 provides a protective strategy against infection and disease. Cell Rep. 26, 906–920 e3.
Tan, C.W., Sam, I.C., Chong, W.L., Lee, V.S., Chan, Y.F., 2017. Polysulfonate suramin inhibits Zika virus infection. Antivir. Res. 143, 186–194.
Tham, H.W., Balasubramaniam, V., Ooi, M.K., Chew, M.F., 2018. Viral determinants and vector competence of Zika virus transmission. Front. Microbiol. 9, 1040.
Toriizuka, Y., Kinoshita, E., Kogure, N., Kitajima, M., Ishiyama, A., Otoguro, K., Yamada, H., Omura, S., Takayama, H., 2008. New lycorine-type alkaloid from Lycoris traubii and evaluation of antitrypanosomal and antimalarial activities of lycorine derivatives. Bioorg. Med. Chem. 16, 10182–10189.
White, M.K., Wollebo, H.S., David Beckham, J., Tyler, K.L., Khalili, K., 2016. Zika virus: an emergent neuropathological agent. Ann. Neurol. 80, 479–489.
Yang, S., Xu, M., Lee, E.M., Gorshkov, K., Shiryaev, S.A., He, S., Sun, W., Cheng, Y.S., Hu, X., Tharappel, A.M., Lu, B., Pinto, A., Farhy, C., Huang, C.T., Zhang, Z., Zhu, W., Wu, Y., Zhou, Y., Song, G., Zhu, H., Shamim, K., Martinez-Romero, C., Garcia-Sastre, A., Preston, R.A., Jayaweera, D.T., Huang, R., Huang, W., Xia, M., Simeonov, A., Ming, G., Qiu, X., Terskikh, A.V., Tang, H., Song, H., Zheng, W., 2018. Emetine inhibits Zika and Ebola virus infections through two molecular mechanisms: inhibiting viral replication and decreasing viral entry. Cell Discov 4, 31.